View metadata, citation and similar papers at core.ac.uk
brought to you by
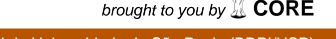
provided by Biblioteca Digital da Produção Intelectual da Universidade de São Paulo (BDPI/USP)

Universidade de São Paulo
Biblioteca Digital da Produção Intelectual - BDPI

Departamento de Física Aplicada - IF/FAP | Artigos e Materiais de Revistas Científicas - IF/FAP

2014-02-21

Gold ion implantation into alumina using an “inverted ion source” configuration.

International Conference on Ion Sources (ICIS 13), 2013, Chiba. Program and Abstracts of the ICIS 13, 2013.
http://www.producao.usp.br/handle/BDPI/44108

Downloaded from: Biblioteca Digital da Produção Intelectual - BDPI, Universidade de São Paulo

Gold ion implantation into alumina using an “inverted ion source” configurationa)

M. C. Salvadori, F. S. Teixeira, L. G. Sgubin, W. W. R. Araujo, R. E. Spirin, M. Cattani, E. M. Oks, and I. G. Brown

Citation: Review of Scientific Instruments **85**, 02B502 (2014); doi: 10.1063/1.4824755
View online: http://dx.doi.org/10.1063/1.4824755
View Table of Contents: http://scitation.aip.org/content/aip/journal/rsi/85/2?ver=pdfcov
Published by the AIP Publishing

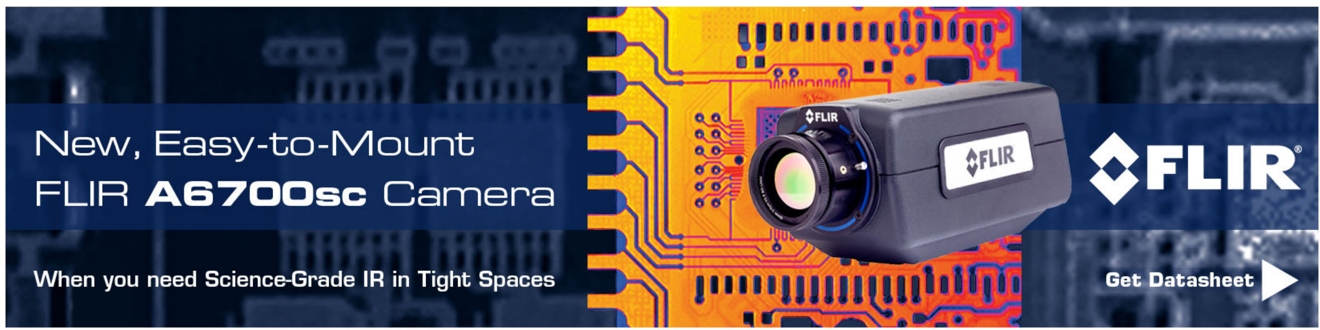

This article is copyrighted as indicated in the article. Reuse of AIP content is subject to the terms at: http://scitationnew.aip.org/termsconditions. Downloaded to IP: 143.107.128.41 On: Fri, 21 Feb 2014 15:56:23

Gold ion implantation into alumina using an "inverted ion source" configuration[a)]

M. C. Salvadori,[1,b)] F. S. Teixeira,[1] L. G. Sgubin,[1] W. W. R. Araujo,[1] R. E. Spirin,[1] M. Cattani,[1] E. M. Oks,[2] and I. G. Brown[3]

[1]*Institute of Physics, University of São Paulo, C.P. 66318, CEP 05315-970, São Paulo, S.P., Brazil*
[2]*High Current Electronics Institute, Russian Academy of Sciences, Tomsk 634055, Russia and National Research Tomsk Polytechnic University, Tomsk 634050, Russia*
[3]*Lawrence Berkeley National Laboratory, Berkeley, California 94720, USA*

(Presented 10 September 2013; received 17 August 2013; accepted 18 September 2013; published online 15 October 2013)

We describe an approach to ion implantation in which the plasma and its electronics are held at ground potential and the ion beam is injected into a space held at high negative potential, allowing considerable savings both economically and technologically. We used an "inverted ion implanter" of this kind to carry out implantation of gold into alumina, with Au ion energy 40 keV and dose (3–9) × 10^{16} cm^{-2}. Resistivity was measured *in situ* as a function of dose and compared with predictions of a model based on percolation theory, in which electron transport in the composite is explained by conduction through a random resistor network formed by Au nanoparticles. Excellent agreement is found between the experimental results and the theory. © *2013 AIP Publishing LLC*. [http://dx.doi.org/10.1063/1.4824755]

I. INTRODUCTION

Energetic ion beams are usually formed by accelerating ions from a plasma held at high positive potential into a space at ground potential, with the ion energy determined by the potential drop through which the ions fall in the beam formation electrode system, $E_i = eQV_{ext}$, where E_i is the final ion energy, e the electron charge, Q the ion charge state, and V_{ext} the extractor voltage drop. An ion implantation system in which the ion source and its electronics could be maintained at ground potential would provide technological and economic advantage. This can be done by maintaining the final grid and the space into which the ion beam is injected at high negative potential. In this case the extractor voltage drop remains high and so also the ion energy, but with the potential profile falling from ground to high negative voltage rather than from high positive voltage to ground. For much laboratory ion implantation, this arrangement offers savings in simplicity and cost that may more than offset the inconvenience of having the target at high voltage. Since the overall device potential profile is the inverse of that usually employed, we call the device an "inverted ion implanter."

We have used our inverted ion implantation facility to explore the surface electrical conductivity of alumina ceramic implanted with gold ions. (We used gold to avoid any uncertainty due to possible oxidation of implanted metal.) Metal ion implanted ceramics are of interest from a fundamental perspective as well as for their applications. An important application of such implanted ceramics is for high-voltage insulators with uniform and designer-determined surface resistivity.[1–6] In prior work Ti and Pt have been used, with implantation dose typically in the mid 10^{16} ions/cm^2 range. High voltage accelerator columns[3,4] and the support rods for electrostatic focusing lenses in single-ion devices[6] have been treated in this way and the results have been highly successful. In these applications, the aim is to bleed off surface charge accumulation, or, said differently, to grade the voltage drop along the component in a uniform and controllable way. Although the approach has met with considerable success, theoretical understanding of the phenomena involved has been lacking.

Here we elaborate on two related topics:

- The inverted ion source, and inverted ion implantation, approach.
- The application of this approach for investigation of the surface resistivity of gold-implanted alumina.

We show that the inverted ion source provides an excellent means for carrying out ion implantation, and that the implantation-induced surface resistivity phenomenon can be described by a model based on percolation theory.

II. EXPERIMENTAL SETUP

In the inverted ion implanter embodiment used here we made use of a vacuum arc to generate metal plasma.[7–9] Gold plasma was formed using a repetitively pulsed, vacuum arc plasma gun with gold cathode, and injected into a bent-solenoid magnetic filter to remove cathode debris from the plasma stream. This plasma facility has been described previously.[10,11] The plasma was directed toward the entrance of the negatively biased implantation chamber. Ion extraction voltage was 20 kV. Ion beam current was monitored by a

[a)]Contributed paper, published as part of the Proceedings of the 15th International Conference on Ion Sources, Chiba, Japan, September 2013.

[b)]Author to whom correspondence should be addressed. Electronic mail: mcsalvadori@if.usp.br

This article is copyrighted as indicated in the article. Reuse of AIP content is subject to the terms at: http://scitationnew.aip.org/termsconditions. Downloaded to IP: 143.107.128.41 On: Fri, 21 Feb 2014 15:56:23

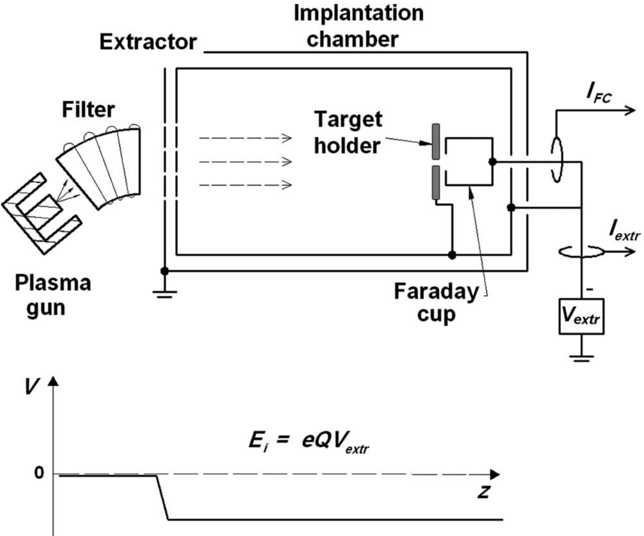

FIG. 1. Schematic of the inverted ion implanter with filtered vacuum arc plasma gun, showing also the on-axis potential profile.

magnetically suppressed Faraday cup, allowing estimation of the implanted dose from the cup current and the number of pulses. The vacuum arc plasma contains multiply stripped ion species.[12,13] For a gold plasma the charge state distribution is Au^{+}:Au^{2+}:Au^{3+} = 14:75:11 (% particle fraction) for a mean charge state Q = 2.0. Thus, the mean gold ion energy (keV) is twice the extraction voltage (kV) − an implantation energy of 40 keV. A schematic of the set up is shown in Fig. 1, and the implantation chamber in Fig. 2.

The advantage of the inverted ion implanter approach as opposed to the conventional approach lies in the great savings in complexity and cost. Figure 3 shows a photograph of the inverted implanter on the bench. The compactness and simplicity of the hardware are evident. The inverted ion source has been described in detail elsewhere,[14] as also its application as an ion implanter.[15]

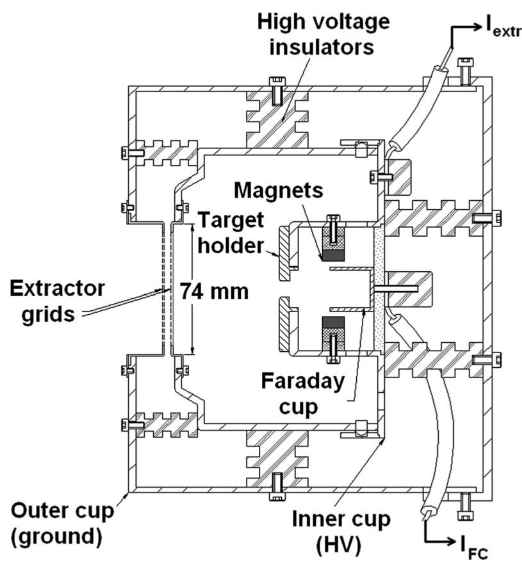

FIG. 2. The beam formation and ion implantation device, showing the extractor grids, outer (ground) chamber and inner (high negative potential) chamber, target holder, and Faraday cup.

FIG. 3. The inverted ion implanter at the Thin Films Laboratory, University of Sao Paulo.

A small alumina sample was positioned near the entrance aperture to the Faraday cup, but not completely covering it, allowing the ion current and thus the implantation dose to be monitored. The surface resistance of the implanted sample was measured *in situ* as the implantation proceeded. For this purpose, electrical contacts were formed at both ends of the substrate with silver paint, and well-insulated leads brought from these contacts to outside the vacuum chamber. After a certain number of pulses of known ion current density, providing a calculable implantation dose, the implantation process was temporarily halted and the resistance of the sample measured; then the implantation was allowed to proceed, and so on, leading to data of resistance *vs.* dose. Transmission electron microscopy (TEM) was performed to visualize the gold nanoparticles that self-agglomerate within the alumina[16] using a Tecnai^{TM} G2 F20 system.

III. RESULTS

The gold implantation depth profile was calculated using the TRIDYN program,[17,18] indicating that the gold distribution peaks at a depth below the alumina surface of about 20 nm for 40 keV and doses 2.5×10^{16} cm^{-2} and 1×10^{17} cm^{-2}. It is known[19] that metal atom concentration above the solubility limit leads to nucleation and growth of metal nanoparticles within the sample. The TEM results provide evidence for gold nanoparticle formation, clearly showing nanoparticles with mean diameter 3.2 nm.[16] A metal/insulator composite layer has been formed.

Electron conduction in disordered media (nanocomposites) can be treated by an "effective medium theory" developed by Kirkpatrick,[20,21] in which the system is considered as a random resistor network. The electrical conductivity σ of the composite is then given by[20]

$$\sigma/\sigma_0 = [(zx/2-1)\sigma_1 + [z(1-x)/2-1]\sigma_2]/(z-2) + [\{(zx/2-1)\sigma_1 + [z(1-x)/2-1]\sigma_2\}^2 + 2(z-2)\sigma_1\sigma_2]^{1/2}/(z-2),$$

This article is copyrighted as indicated in the article. Reuse of AIP content is subject to the terms at: http://scitationnew.aip.org/termsconditions. Downloaded to IP: 143.107.128.41 On: Fri, 21 Feb 2014 15:56:23

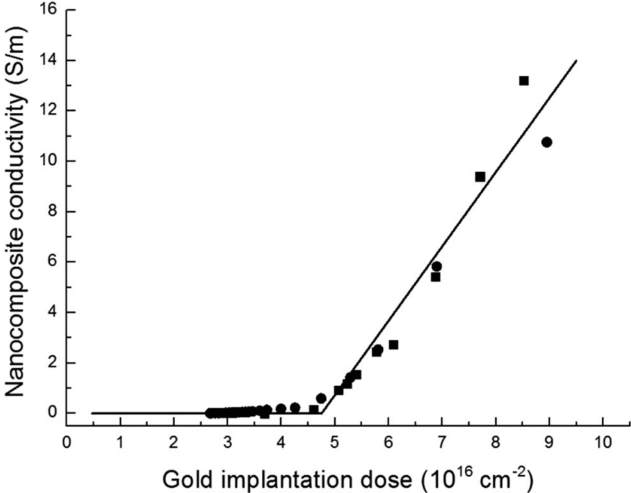

FIG. 4. Measured conductivity *vs.* implantation dose for Au-implanted alumina (two independent runs, shown as circles and squares). The solid line is the theoretical prediction.

where σ_0 is the saturation conductivity for which the material still remains a composite, z is the number of bonds at each node of the network, σ_1 is the conductivity of the conducting material, σ_2 is the conductivity of the insulating material, and $x = \varphi/\varphi_0$ is the normalized metal atom concentration, where φ is the implantation dose and φ_0 is the saturation dose (the maximum dose for which the material still remains a composite); for doses greater than φ_0, a metal film is deposited on the insulator surface and the material takes on the characteristics of a thin metal film.

Figure 4 shows the theoretical calculation as a continuous curve and the experimental results as squares and circles (two separate samples, indicating the reproducibility of the results). The model describes the experimental resistivity results very nicely. The saturation conductivity, σ_0, and the maximum dose, φ_0, for which the Au/alumina system remains an insulator/conductor composite, were 14 S/m and 9.5 $\times$ 10^{16} cm^{-2}, respectively; and the percolation dose φ_c (the critical concentration below which the composite has the same conductivity as the insulating host material) was 4.4×10^{16} cm^{-2}.

IV. CONCLUSION

The inverted ion source and its application as an inverted ion implanter described here provide technological simplicity and economic savings to the challenge of setting up an ion implantation research facility. We have demonstrated the value of the approach as a research tool by carrying out gold ion implantation into alumina, at an ion energy of 40 keV and implantation dose up to the high 10^{16} cm^{-2}.

The surface resistivity of gold-implanted alumina was measured *in situ* as a function of implantation dose and the results compared to a theory based on percolation – conduction within the random resistor network formed by a buried layer of gold nanoparticles within the alumina – an excellent agreement was found. Percolation provides a good model for the mechanism of conductivity in metal ion implanted ceramics. A more comprehensive paper, describing both the detailed experimental results and the percolation theory to which the results are compared, has been published.[16]

ACKNOWLEDGMENTS

This work was supported by the Fundação de Amparo a Pesquisa do Estado de São Paulo (FAPESP) and the Conselho Nacional de Desenvolvimento Científico e Tecnológico (CNPq), Brazil. We are grateful to the Institute of Ion Beam Physics and Materials Research at the Forschungszentrum Dresden-Rossendorf, Germany, for the TRIDYN-FZR computer simulation code.

[1] Y. C. W. White, C. J. McHargue, P. S. Sklad, L. A. Boatner, and G. C. Farlow, Mater. Sci. Eng. R. **4**, 41 (1989).
[2] S. Anders, A. Anders, and I. Brown, in Proceedings of the IEEE 1993 Particle Accelerator Conference, Washington, DC, 17–20 May 1993.
[3] F. Liu, I. Brown, L. Phillips, G. Biallas, and T. Siggins, in *Proceedings of the IEEE Particle Accelerator Conference*, Vancouver, BC, Canada, 12–16 May 1997.
[4] F. Liu, M. R. Dickinson, R. A. MacGill, A. Anders, O. R. Monteiro, I. G. Brown, L. Phillips, G. Biallis, and T. Siggins, Surf. Coat. Technol. **103–104**, 46 (1998).
[5] D. Li, J. Zhang, M. Yu, J. Kang, and W. Li, Appl. Surf. Sci. **252**, 1029 (2005).
[6] A. Nikolaev, E. M. Oks, K. Savkin, G. Yu. Yushkov, D. J. Brenner, G. Johnson, G. Randers-Pehrson, I. G. Brown, and R. A. MacGill, Surf. Coat. Technol. **201**, 8120 (2007).
[7] *Handbook of Vacuum Arc Science and Technology*, edited by R. L. Boxman, D. M. Sanders, and P. J. Martin (Noyes, Park Ridge, NJ, 1995).
[8] A. Anders, *Cathodic Arcs: From Fractal Spots to Energetic Condensation* (Springer, New York, 2008).
[9] I. G. Brown, "Cathodic arc deposition of films," Annu. Rev. Mater. Sci. **28**, 243 (1998).
[10] D. R. Martins, M. C. Salvadori, P. Verdonck, and I. G. Brown, Appl. Phys. Lett. **81**, 1969 (2002).
[11] M. C. Salvadori, L. L. Melo, A. R. Vaz, R. S. Wiederkehr, F. S. Teixeira, and M. Cattani, Surf. Coat. Technol. **200**, 2965 (2006).
[12] I. G. Brown and X. Godechot, IEEE Trans. Plasma Sci. **19**, 713 (1991).
[13] I. Brown and E. Oks, IEEE Trans. Plasma Sci. **33**, 1931 (2005).
[14] M. C. Salvadori, F. S. Teixeira, L. G. Sgubin, W. W. R. Araujo, R. E. Spirin, E. M. Oks, and I. G. Brown, Rev. Sci. Instrum. **84**, 023506 (2013).
[15] M. C. Salvadori, F. S. Teixeira, L. G. Sgubin, W. W. R. Araujo, R. E. Spirin, E. M. Oks, K. M. Yu, and I. G. Brown, Appl. Phys. Lett. **101**, 224104 (2012).
[16] M. C. Salvadori, F. S. Teixeira, L. G. Sgubin, M. Cattani, and I. G. Brown, Nucl. Instrum. Methods Phys. Res. B **310**, 32 (2013).
[17] W. Möller and W. Eckstein, Nucl. Instrum. Methods Phys. Res. B **2**, 814 (1984).
[18] W. Möller, W. Eckstein, and J. P. Biersack, Comput. Phys. Commun. **51**, 355 (1988).
[19] A. L. Stepanov, D. E. Hole, and P. D. Townsend, J. Non-Cryst. Solids **260**, 65 (1999).
[20] S. Kirkpatrick, Phys. Rev. Lett. **27**, 1722 (1971).
[21] S. Kirkpatrick, Rev. Mod. Phys. **45**, 574 (1973).

This article is copyrighted as indicated in the article. Reuse of AIP content is subject to the terms at: http://scitationnew.aip.org/termsconditions. Downloaded to IP: 143.107.128.41 On: Fri, 21 Feb 2014 15:56:23